Since the frozen speed of sound usually is greater than the equilibrium value, the frozen speed becomes identified with the wave front (see Moore and Gibson[12, 13]).

References

[1] Brinkley, S. R., Jr. and Kirkwood, J. G., "On the condition of stability of the plane detonation wave," *Third Symposium on Combustion, Flame, and Explosion Phenomena* (Williams and Wilkins Company, Baltimore, Md., 1949), p. 586.

[2] Brinkley, S. R., Jr. and Richardson, J. M., "In the structure of plane detonation waves with finite reaction velocity," *Fourth Symposium (International) on Combustion* (Williams and Wilkins Co., Baltimore, Md., 1953), p. 456.

[3] Kirkwood, J. G. and Wood, W. W., "Structure of a steady-state plane detonation wave with finite reaction rate," J. Chem. Phys. **22**, 1915–1919 (1954).

[4] Munk, M. M., "Remarks on the velocity of sound," J. Aeronaut. Sci. **22**, 795 (1955).

[5] Resler, E. L., Jr., "Sound speed in a reacting medium," J. Chem. Phys. **25**, 1287–1288 (1956).

[6] Resler, E. L., Jr., "Sound speed," J. Chem. Phys. **27**, 596–597 (1957).

[7] Resler, E. L., Jr., "Characteristics and sound speed in nonisentropic gas flows with nonequilibrium thermodynamic states," J. Aeronaut. Sci. **24**, 785–790 (1957).

[8] Wood, W. W. and Kirkwood, J. G., "Characteristic equations for reactive flow," J. Chem. Phys. **27**, 596 (1957).

[9] Chu, B.-T., "Wave propagation in a reacting mixture," *1958 Heat Transfer and Fluid Mechanics Institute* (Stanford University Press, Stanford, Calif., 1958), pp. 80–90.

[10] Mirels, H., "Comments on characteristics and sound speed on nonisentropic gas flows with nonequilibrium thermodynamic states," J. Aerospace Sci. **25**, 460–461 (1958).

[11] Resler, E. L., Jr., "Author's reply," J. Aerospace Sci. **25**, 461 (1958).

[12] Moore, F. K., "Propagation of weak waves in a dissociated gas," J. Aeronaut. Sci. **25**, 279–280 (1958).

[13] Moore, F. K. and Gibson, W. E., "Propagation of weak disturbances in a gas subject to relaxation effects," J. Aerospace Sci. **27**, 117–128 (1960).

Surface Temperatures Due to Localized Removal of a High-Emittance Coating on the Thin-Plate Sections of a Re-Entry Vehicle

FRITZ R. S. DRESSLER*

Ballistic Research Laboratories, Aberdeen Proving Ground, Md.

Nomenclature

T = temperature
T_{ab} = adiabatic wall temperature
T_j = equilibrium temperature appropriate to $\epsilon_j (j = 1,2)$
r = length of radius vector
ϵ = emittance
H = heat transfer coefficient
k = conductivity of plate
t = plate thickness (necessarily small)
σ = Stefan-Boltzman constant
β_j = $[4\epsilon_j \sigma T_j^3 + H_j]/kt\ (j = 1,2)$
C_1 = $K_1/[K_1 I_0 + (\beta_1/\beta_2)^{1/2} K_0 I_1]$
C_2 = $I_1/[K_0 I_1 + (\beta_2/\beta_1)^{1/2} K_1 I_0]$
C_3 = $1/\{\cosh[(\beta_1)^{1/2} S] + (\beta_1/\beta_2)^{1/2} \sinh[(\beta_1)^{1/2} S]\}$
C_4 = $1/\{1 + (\beta_2/\beta_1)^{1/2} \coth[(\beta_1)^{1/2} S]\}$
I_0 = modified Bessel function of first kind, zero order
I_1 = modified Bessel function of first kind, first order
K_0 = modified Bessel function of second kind, zero order
K_1 = modified Bessel function of second kind, first order
I's have the argument $[(\beta_1)^{1/2} R]$; the K's, $[(\beta_2)^{1/2} R]$

Received February 11, 1963.

* Mathematician.

CONSIDER an element of surface ΔA exposed to high-speed flow. The fundamental equations are developed by noting the following: 1) energy radiated away from the element = $\epsilon\sigma T^4 \Delta A$; 2) energy convected to the surface = $H(T_{ab} - T)\Delta A$; 3) energy conducted into the volume beneath ΔA (the temperature through the plate is essentially constant) = $kt\nabla^2 T \Delta A$.

Consider steady-state conditions: i.e., $\dot{T} \equiv 0$. The foregoing considerations give

$$\nabla^2 T = (\epsilon\sigma/kt)T^4 - (H/kt)(T_{ab} - T) \qquad (1)$$

Let a small circular area of radius $r = R$ have a lower emittance than the rest of the plate. Now suppose for a moment that no energy is transmitted (conducted) between this low emittance area $0 \leq r \leq R$ and the rest of the plate. The temperature on the plate is T_2 and, on the low emittance area, $T_1 (\epsilon_1 < \epsilon_2)$. When $(T_1 - T_2)/T_j$ $(j = 1,2)$ is small, it is said that, if energy were allowed to be transmitted, the new steady-state temperature profile that would establish itself could not differ greatly from the previous equilibrium temperature profile. In view of this, one can write

$$T = T_j + T_j' \qquad (j = 1,2)$$

where T_j' is a small quantity with respect to T_j. Incorporating the foregoing discussion into Eq. (1),

$$\nabla^2 T_j' = (1/kt)(4\sigma\epsilon_j T_j^3 + H_j) T_j' \qquad (2)$$

where terms of order $(T_j'/T_j)^2$ and higher have been neglected.

Based on a polar coordinate system placed at the center of the circular area, Eq. (2) is solved separately in region $0 \leq r \leq R (j = 1)$ and in region $r > R (j = 2)$. The separate solutions then are matched at $r = R$. The resulting solutions, satisfying all boundary conditions, can by given. For $0 \leq r \leq R$,

$$T = T_1 - C_1(T_1 - T_2) I_0[(\beta_1)^{1/2} r] \qquad (3)$$

For $r > R$,

$$T = T_2 + C_2(T_1 - T_2) K_0[(\beta_2)^{1/2} r] \qquad (4)$$

The equation of interest is Eq. (3). It is found that, in all applications, the argument of I_0 is small, i.e., $I_0 \approx 1$ for values of $0 \leq r \leq R$. This permits one to write

$$T \approx T(0) = T_1 - C_1(T_1 - T_2) \qquad (5)$$

for the hot circular area.

Equation (2) may be used also in the case of a long, narrow (length/width $\gg$ 1) area of low emittance. Based on a rectangular Cartesian coordinate system located at the center of the long strip (y axis along the strip), Eq. (2) is solved similarly to the polar case. The resulting solutions, satisfying all boundary conditions, can be given. For $0 \leq x \leq S$ = semiwidth of strip,

$$T = T_1 - C_3(T_1 - T_2) \cosh[(\beta_1)^{1/2} x] \qquad (6)$$

For $x > S$,

$$T = T_2 + C_4(T_1 - T_2) \exp[(\beta_2)^{1/2}(S - x)] \qquad (7)$$

The equation of interest is Eq. (6). The temperature of the strip can be approximated by

$$T \approx T(0) = T_1 - C_3(T_1 - T_2) \qquad (8)$$

A comparison of Eqs. (5) and (8) reveals that, for similar conditions, the narrow strip is critical. In other words, a long scratch of width $2S$ will be hotter than a circular spot of diameter $2R$ where $S = R$.

Note that Eq. (2) is valid for the following cases:

$$\epsilon_1 \neq \epsilon_2 \quad \epsilon_1 = \epsilon_2 \quad \epsilon_1 \neq \epsilon_2$$
$$H_1 = H_2 \quad H_1 \neq H_2 \quad H_1 \neq H_2$$

That is, the foregoing analysis can be extended to the case of a high (low) local heat transfer coefficient.

Double-Shock Shock Tube for Simulating Blast Loading in Supersonic Flow

Bo Lemcke*
Massachusetts Institute of Technology, Cambridge, Mass.

EXPERIMENTAL simulations of blast loading on moving bodies have been performed mainly in shock tubes until now. Although capable of producing strong shock waves, the shock tube has not been used to establish the interaction between the blast wave and an initial flow on a body. This note will describe a method for obtaining both the initial flow and a blast wave in a shock tube.

It was found by the author[1] that when using a configuration like that shown in Fig. 1, with a large area driver, separated from the shock tube by a diaphragm downstream of the area change, two shock waves appeared at the end of the shock tube. The pressure records obtained were similar to the pressure history indicated on Fig. 2. The explanation for the second shock wave is as follows. When the diaphragm bursts an expansion fan propagates upstream towards the area change. Because of the further supply of driving energy, the rarefaction waves will be reflected as compression waves from the area change, see Fig. 1. The compression waves will converge into a shock wave which will be swept down the expansion tube by the already moving gas. The last compression wave will be generated when the flow in the contraction reaches sonic speed. The further compression behind the second shock wave, indicated in Fig. 2, is due to the arrival of compression waves that have not yet caught up with the shock wave.

To improve the strength and shape of the second shock wave further, it is proposed that another diaphragm be introduced, located at the area change, Fig. 3. This additional diaphragm would make it possible to use different gases and pressures in the two sections of the driver. The configuration utilizing two diaphragms will be called a double-shock shock tube and the different sections the driver, the intermediate driver, and the expansion tube, respectively (see Fig. 3).

The wave pattern in a double-shock shock tube would be slightly different in the early stages from that shown in Fig. 1. It is assumed that the pressure in the driver is of the same order as that in the intermediate driver and that the second diaphragm, located at the area change, cannot withstand a pressure difference that is equal to the pressure in the driver. When the first diaphragm bursts, a rarefaction fan H-T will propagate, as before, up toward the area change. Now, however, it will be reflected from the second diaphragm as a rarefaction wave, thus causing the pressure at the diaphragm to decrease rapidly and eventually forcing it to burst. Thus the second shock wave, S_2, will be formed almost instantaneously at the entrance to the shock tube. If the strength of the second diaphragm is chosen so that the throat becomes sonic immediately, there will be no compression waves following the second shock wave. Thus the introduction of the second diaphragm is expected to make it possible to obtain a well defined second shock wave at a suitable position in the expansion tube. The regulation of the time difference between the two shock waves is affected simply by varying the ratio between the lengths of the intermediate driver and the expansion tube. The flow behind the first shock wave can be used now for establishing steady subsonic or supersonic flow around a body, and the second shock wave can serve as the blast wave for studying the blast loading and the blast wave-bow shock wave interaction.

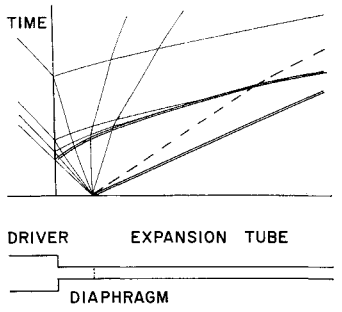

Fig. 1 Configuration used for obtaining two shock waves and the corresponding wave pattern

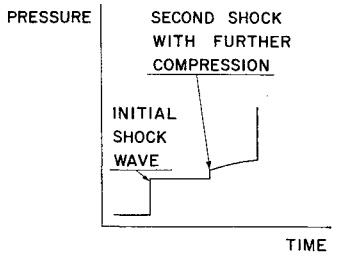

Fig. 2 Obtained pressure record with the configuration indicated in Fig. 1

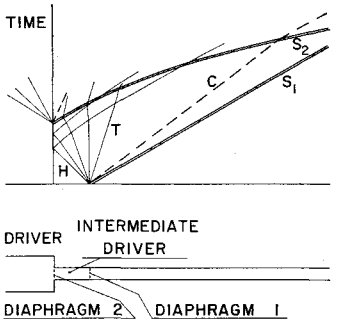

Fig. 3 Wave pattern in double-shock shock tube

To show the capability of the double-shock shock tube one particular case has been worked out by the method of characteristics. The initial conditions were, driver gas: combustion products of 8 He + 3 H_2 + O_2 at 3000 atm;[2] intermediate driver: hydrogen at 2000 atm and 300°K; driver gas: air at 0.2 atm and 300°K. The combustion was assumed to be complete when diaphragm 1 ruptured. Diaphragm 2 was assumed to burst for a pressure difference exactly sufficient to produce a sonic throat at the area change. Real gas effects were taken into account for the shock waves in air. The main results of the calculation were as follows: the stagnation pressure and temperature on a model in the initial flow were 165 atm and 5700°K, respectively; the pressure ratio over the second shock wave after its interaction with the contact surface, C in Fig. 3, was 7.70; the total testing time between the arrival at the end of the shock tube of the first shock wave and the contact surface was about 600 μsec for a 100-ft-long expansion tube.

By changing the gases and pressures in the different sections of the double-shock shock tube a wide range of stagnation conditions on the model as well as blast wave strengths can be simulated. Although the Mach number in the initial flow will be limited to about three, stagnation conditions on the model corresponding to very high velocities at low altitudes can be obtained. Thus the importance of real gas

Received February 25, 1963.

* Senior Research Engineer, Aeroelastic and Structures Research Laboratory.